



Research Article

INVESTIGATION OF MECHANICAL AND METALLOGRAPHIC PROPERTIES OF TWO DIFFERENT ALUMINUM ALLOYS JOINED WITH FRICTION STIR WELDING METHOD USING DIFFERENT WELDING PARAMETERS

Şeref ÖCALIR¹, Uğur EŞME², Cem BOĞA*³, Mustafa Kemal KÜLEKÇİ⁴

¹*Automotive Engineering, Tarsus University, MERSİN; ORCID: 0000-0003-0123-2295*

²*Automotive Engineering, Tarsus University, MERSİN; ORCID: 0000-0002-0672-7943*

³*Mechanical Engineering, Adana Alparslan Türkeş Science and Technology University, ADANA; ORCID: 0000-0002-9467-1141*

⁴*Automotive Engineering, Tarsus University, MERSİN; ORCID: 0000-0002-5829-3489*

Received: 31.03.2020 Revised: 23.04.2020 Accepted: 25.04.2020

ABSTRACT

In this study two aluminum alloy materials of EN AW-5083-H111 and EN AW-6082-T651 were joined with Friction Stir Welding considering the parameters as the tool shoulder diameter, spindle speed and feed rate. The mechanical properties of the weld joints such as yield strength, tensile strength and micro-hardness and metallographic properties were investigated comparatively with the use of these welding parameters. The yield strength of the weld joints were determined to be between 136-217 MPa while the tensile strengths were between 159-230 MPa and the percent elongations were between 2.28-5.44 %. The hardness values measured in weld areas were higher in the EN AW-6082 base metal side compared with EN AW-5083 base metal side.

Keywords: Aluminum alloy, friction stir welding (FSW), mechanical properties, metallographic properties.

1. INTRODUCTION

With technological advances, the rise in human needs have become inevitable. Mankind needed new inventions and new materials to be used in the construction of these inventions in every period of history in order to meet these needs. Today, with the advances of technology, there have also been improvements in joining of metal-based materials with welding. Welding is a method of joining materials through the application of heat or pressure or with the application of both. In most welding processes there is a high heat input to the material. In fusion welding methods which utilize heat, the heated metals tend to oxidize. Therefore, when welding metals which are more eager to make compounds with oxygen, it is needed to take the required precautions [1-4]. Aluminum alloys are one of the materials that are difficult to join with fusion welding methods. This is caused by poor mechanical properties due to melting and recasting structure in weld zone and low hardness of Al alloys, physical properties of aluminum and its affinity to oxygen. Tungsten inert gas (TIG), metal inert gas (MIG), resistance welding, laser

* Corresponding Author: e-mail: cboga@atu.edu.tr, tel: (322) 455 00 00 / 2188

welding, electron beam welding and plasma arc welding (PAW) are fusion welding methods commonly used for joining aluminum alloys. Since these welding methods involve melting and subsequent solidification, undesirable microstructural changes take place in the structure of aluminum alloys and high magnitude of distortions occur in the heat affected zones (HAZ). In addition, significant decrease in hardness and losses in mechanical properties are observed in HAZ. However, friction stir welding (FSW), a solid state joining process, is used as an alternative welding method in joining non-ferrous metals, especially aluminum alloys [5-9]. The ship and maritime industry was one of the first to use the FSW method commercially. FSW method is used to assemble deck and side partitions and floor panels, hull and superstructures, helicopter landing platforms, cooling facilities for the ship and maritime industry [10]. FSW method provides great weight reduction compared to traditional riveting method for the fuselage section of the aircrafts. FSW applications are seen in the skins of wings and fuselage structures for the use of commercial and military aircrafts [11]. FSW process presents significant advantages for reducing cost and weight in contrast to riveting. Today, FSW is used commercially by many automotive companies and suppliers. FSW is also used in joining aluminum alloy parts manufactured with extrusion methods to be used in commercial production of high speed trains. [12]. When the literature is reviewed there are many publications regarding the investigation of mechanical properties, micro structures and corrosion specifications of welded joints of aluminum alloys bonded with each other or with various metal alloys with respect to the alteration of welding parameters. The publications which investigate the mechanical properties, microstructures and corrosion behaviours of welded joints using FSW method for joining the aluminum alloys AA 5083 and AA 6082, which were also used in this study, can be summarized as follows; James et al. [13], investigated the fatigue behaviour, hardness, macro and micro structural specifications of welded joints of the aluminum alloy AA 5083-H321, which is suitable for maritime applications, welded at travel speeds ranging from 80 mm/min – 200 mm/min. As a result of their work, they determined that when welding travel speed increases, the fatigue life decreases. Even though it's rare they detected porosity in the welded joints and they indicated that these defects initiate crack formation. Kumar et al. [14] aimed to make a full factorial design study about welding parameters and by using statistical approaches they tried to develop experimental relations. As a result of their study concerning the joining of Al 5083 alloy with FSW method, they indicated that spindle speed, feed rate, tool shoulder diameter and pin diameter are critical factors affecting the heat input and forces that occur in the FSW process. They also determined that tool shoulder diameter, spindle speed and feed rate are factors that affect the axial force. Cavaliere et al. [15] joined AA 6082 aluminum alloy plates of 4 mm thickness with FSW method and investigated the effect of various feed rates on the mechanical properties and micro structures of weld joints. In their study with 6082 aluminum alloy, Mroczka and Pietras [16] performed FSW applications in various welding speeds and utilized additional cooling operations. They examined the microstructures and mechanical properties of the welded joints. As a result, it was observed that there was a zigzag pattern in the welded area. They concluded the zigzag pattern was formed due to the mixing of the oxide layer into the welded area. In their study, Costa et al. [17], examined the fatigue strength of friction stir weld joints of AA 6082-T6 alloys both experimentally and predictively in various spectrums. They reported that the tunnel defects that are formed as a result of the welding process decrease the fatigue life. They observed that the mentioned tunnel defects have higher influence on the fatigue life than the shear lips stress concentration that occur after the welding process. El-Danaf and El-Rayes [18] joined AA 6082 Al alloys with FSW using different welding parameters and investigated the mechanical properties and microstructures of the weld joints. Additionally, they applied heat treatment to the welded joints and observed the microstructural changes. As a result of their study, they observed noticeable decrease of hardness in the weld zone and especially in the thermo-mechanically affected zone (TMAZ). In their study regarding the joining of cold wrought aluminum alloys with the FSW method, El-Rayes and El-Rayes [19] investigated the effect of feed rate and multi pass application on the mechanical

properties and micro-structures of the weld zone. In their work about the joining of AA 6082 alloys, Cabibbo et al. [20] carried out FSW method employing various technological configurations. In the scope of the study, they investigated the microstructural specifications of the welded joints acquired with double sided FSW method compared to the welded joints obtained with single sided FSW method. Krasnowski et al. [21] investigated the effects of different tool shapes and tool configurations on the mechanical properties and microstructure of FSW welded joints. They observed that different tool designs affected the tensile strength and micro-hardness of the weld area. In the study it was also concluded that double sided FSW welds showed poor mechanical properties than that of single-sided FSW welds due to the increased heat input to the weld area. Cho et al. [22] joined A5083 and A6082 alloys in various welding circumstances and evaluated the microstructures and mechanical properties of the welded joints. As a result of their work they noticed variation in grain size and crystalline structure in the welding area and also they observed equiaxed grain structure in the weld zone due to dynamic recrystallization during FSW. According to the temperature measurements realized during the welding process it was reported that they gathered similar temperature values for both alloys. Singh and Shankar [23] joined 5083 and 6082 aluminum alloys of 6 mm thickness using parameters such as various spindle speeds, various feed rates, various pin profiles and various tool shoulder diameters. As a result of their study they reported that there was a 10% increase of hardness in the welding area and the optimum performance could be reached by utilizing a tool having a large diameter, high spindle speed and a pin with a circular shape. Gungor et al. [24] joined 5083-H111 and 6082-T651 aluminum alloy plates with each other and with different alloys. A spindle speed of 1250 rpm, a feed rate of 64 mm/min and a tool slope angle of 2° was used as the welding parameters. As a result of their work they reported an 86% welding performance for the 5083-H111 alloy. As a result of the optical microscope and scanned electron microscope observations, no weld defects were found in the welding area. Zucchi et al. [25] compared the pitting and stress corrosion cracking resistance properties of AA5083 aluminum alloys welded with FSW method with that of the joints welded with MIG welding method. They observed that the pitting and stress corrosion cracking resistance properties of weld joints were superior to properties of the base metal itself. They also suggested that FSW welded joints were not prone to stress corrosion cracking while MIG weld joints cracked during tests. In their study which investigates the corrosion behaviour of AA5083-H111 alloy, Vilaca et al. [26] examined the hardness profiles and microstructures of weld beads. They observed that the small unifications in grains and reductions in precipitations at the HAZ and TMAZ, played a vital role in preventing corrosion development. Park et al. [27] studied to determine the optimum environment conditions for the corrosion protection of AA 5083-O aluminum alloys in seawater conditions. The results of the potentiostatic tests showed that the weld joints had low current density and showed optimum level of corrosion resistance between -1.5 and -0.7 V potentials. In addition to that, in situations where the galvanic cell form is provided in the weld joints, a stable structure against corrosion can be obtained. Shen et al. [28] investigated microstructures and corrosion behaviours of FSW welded joints of 5083/6082 aluminum alloys. In their study they compared the results of galvanic tests, potentiodynamic polarization curve tests and electrochemical impedance tests of welded joints against the base materials. After the tests, the observations revealed that using the chosen parameters, the welded joints showed less average corrosion rates than that of the base materials. Patil and Soman [29] examined the corrosion behaviours of 6082-T6 aluminum alloy plates welded with various FSW parameters such as feed rate and different pin profiles. They determined that the decrease in feed rate creates an improvement on corrosion resistance in weld joints. They also reported that the weld joints obtained by the use of the hexagon pin profile had the best corrosion resistance among all the weld joints obtained with other pin profiles. Donatus et al. [30] studied the corrosion susceptibility of AA 5083-O and AA 6082-T6 alloys welded with FSW. In the scope of their study, they compared two different feed rate values and detected that the weld joints made with the higher feed rate showed more susceptibility to corrosion.

In this study, firstly, AA 5083 and AA 6082 aluminum alloys were joined with various different FSW parameters. After the joints were obtained, test specimens conforming to the standards were prepared and the mechanical properties of the weld joints were tested and micro and macro structures were examined. Metallographic analyses were realized by observing the scanning electron microscope (SEM) images. Mechanical tests and results from structural examinations of the weld joints were discussed with graphics in the results and discussions section.

2. MATERIALS AND METHODS

2.1. Aluminum alloy materials

In this study, due to their high corrosion resistance, perfect ductility, good malleability and good weldability properties EN AW-5083-H111 and EN AW-6082-T651 Aluminium alloy plates of 4 mm thickness were used. Chemical compositions of the mentioned aluminum alloys are given in Table 1 and physical and mechanical properties of the alloys are given in Table 2.

Table 1. Chemical composition of Aluminium alloys [31]

Chemical properties	Si	Cr	Mn	Mg	Cu	Ti	Fe	Zn	Al
EN AW-5083-H111	0.00-0.40	0.05-0.25	0.40-1.00	4.00-4.90	0.00-0.10	0.00-0.15	0.00-0.40	0.00-0.25	remainder
EN AW-6082-T651	0.70-1.30	0.00-0.25	0.40-1.00	0.60-1.20	0.00-0.10	0.00-0.10	0.00-0.50	0.00-0.20	remainder

Table 2. Mechanical and physical properties of alloys [31, 32]

Mechanical Properties	EN AW-5083-H111	EN AW-6082-T651
Yield strength (MPa)	170	200-260
Tensile strength (MPa)	310	270-310
Elongation (%)	17	6-8
Elasticity modulus (GPa)	71	70
Physical Properties		
Density (g/cm ³)	2.66	2.70
Melting temperature (°C)	574	555
Coefficient of thermal expansion (1/K)	23.9x10 ⁻⁶	23.4x10 ⁻⁶
Thermal capacity (W/m.K)	120	170-220

2.2. Application of FSW method

Semi-automatic milling machine with a motor power of 4.8 kW and a course length of 1200 mm was used in the FSW process at the fundamental manufacturing laboratory of Tarsus University Faculty of Technology. (Fig. 1a). Procured plates of 4 mm thickness were cut into smaller sizes with guillotine shear machine and the plates were sized to 125 mm x 400 mm dimensions with the help of a milling machine. The plates were welded with the FSW method in butt weld position using three different tool shoulder diameters, three different spindle speeds and three different feed rates.

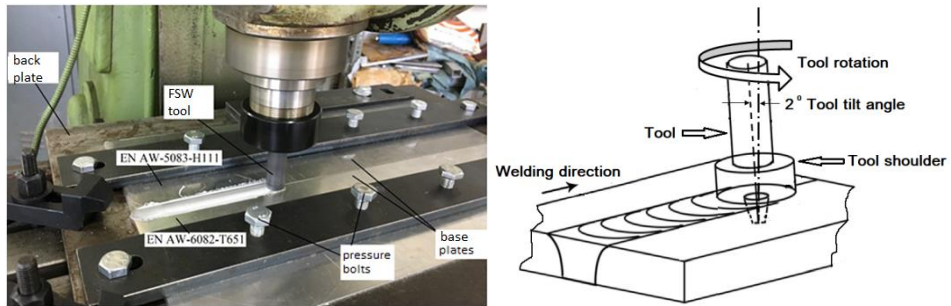


Figure 1. a) Application of FSW process b) Schematic representation of tool

Table 3. Welding parameters and parameter codes

Runs	Tool shoulder diameter (mm)	Spindle speed (min-1)	Feed rate (mm/min)	Parameter codes	
1.	16	710	56	1-T16-S710-F56	
2.			112	2-T16-S710-F112	
3.			160	3-T16-S710-F160	
4.		1000	1400	56	4-T16-S1000-F56
5.				112	5-T16-S1000-F112
6.				160	6-T16-S1000-F160
7.		1400	1400	56	7-T16-S1400-F56
8.				112	8-T16-S1400-F112
9.				160	9-T16-S1400-F160
10.	20	710	56	10-T20-S710-F56	
11.			112	11-T20-S710-F112	
12.			160	12-T20-S710-F160	
13.		1000	1400	56	13-T20-S1000-F56
14.				112	14-T20-S1000-F112
15.				160	15-T20-S1000-F60
16.		1400	1400	56	16-T20-S1400-F56
17.				112	17-T20-S1400-F112
18.				160	18-T20-S1400-F160
19.	24	710	56	19-T24-S710-F56	
20.			112	20-T24-S710-F112	
21.			160	21-T24-S710-F160	
22.		1000	1400	56	22-T24-S1000-F56
23.				112	23-T24-S1000-F112
24.				160	24-T24-S1000-F160
25.		1400	1400	56	25-T24-S1400-F56
26.				112	26-T24-S1400-F112
27.				160	27-T24-S1400-F160

16 mm, 20 mm and 24 mm diameter tools were used as tool shoulder diameter. The spindle speeds of 710 rpm, 1000 rpm and 1400 rpm were assigned. When the rotational speed exceeded 1400 rpm the milling machine showed contactor fault. Hence the maximum rotational speed value was determined as 1400 rpm. The specified spindle speed values are in the range consistent with

the literature. Feed rate values were chosen as 56 mm/min, 112 mm/min and 160 mm/min. In Table 3 FSW process made in 27 runs, parameters and parameter codes are given. Regarding the parameter codes, T represents tool shoulder diameter, S represents spindle speed and F represents feed rate.

The welding process was applied in four steps. In the first step the tool was plunged between the two work pieces until sufficient pressure was attained, in the second step was the waiting period until the materials to get softened, the third step was advance phase and the fourth step was the removal of the tool from the material. A 2° tool tilt angle was used (Fig. 1b). This angle prevented any material removal from the surface during the welding process. The tool dwelled on the base metal surface for 60 seconds before the travel of the tool began. This dwell time was determined in order to generate the required heat for the welding process. During the welding process the tool rotated in clockwise and the EN AW-5083- H111 aluminum alloy was positioned on the advancing side while the EN AW-6082-T651 aluminum alloy was positioned on the retreating side.

2.3. Preparation of the test specimens after the FSW process

The test specimens were prepared according to the EN ISO 6892-1 (Metallic materials - Tensile testing - Part 1: Method of test at room temperature). After being cut by a band saw, the specimens were machined to their final dimensions with a milling machine. Two test specimens were prepared for every welding parameter investigated in the study. The test specimens prepared according to the tensile test standards are shown in Fig. 2. The tensile test was carried out at room temperature with a 1 mm/min speed.



Figure 2. Test specimens prepared according to EN ISO 6892-1 Standard

In order to evaluate the hardness properties with micro-examinations of the welded areas, test samples were taken to cover 10 mm more than the shoulder width of the tool. The specimens were molded with polyester resin. The specimens were sanded and polished successively in the exact order of 240-320-400-600-800-1000-1200-1500-1800 and 2000 grit SiC waterproof sand papers. Polisher has two platens with variable speed range in polishing machine. One disc can be used for grinding while the other disc can be used for polishing. The specimens were polished using disks and cloths with water suspension of 3 µ and 1 µ diamond particles. Following the polishing process the surfaces were soaked in a solution prepared with 25 ml methanol, 25 ml hydrochloric acid, 25 ml nitric acid and 1 drop of hydrofluoric acid for 60 seconds. After that the specimens were washed with distilled water. The specimens that were used in hardness measurements are shown in Fig. 3.

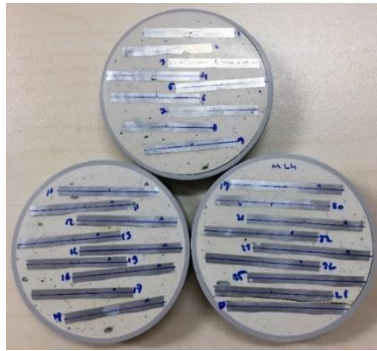


Figure 3. Specimens used for hardness measurement

Micro hardness measurements were taken from weld joint sections using a Vickers hardness measurement device. Measurements were taken starting from the weld center with 1 mm distances. 200 gr load applied for 15 seconds in hardness measurements.

3. RESULTS AND DISCUSSION

In the visual inspections of the FSW joints no distortions were observed on the welded plates due to the limited heat input. When large shoulder diameter and high spindle speed were employed as welding parameters, it was observed that this caused the weld surface to deteriorate. When small shoulder diameter and high spindle speed were employed, it was observed that better joint surface were formed.

3.1. Tensile test findings

The tensile test was applied to two specimens of every plate welded using 27 various parameters. Following the tensile tests of weld joints, the resulting average values of yield strength, tensile strength and % elongation were determined.

The tensile test results belonging to the plates welded using 27 various parameters were given in Table 4. When the tensile test results are examined, it is observed that the yield strength values of weld joints generally are above the yield strength values of EN AW-5083-H111 base metal while the tensile strength values of weld joints were below the tensile strength values of both of the base metals. The yield strength of the weld joints were between 136-217 MPa, the tensile strength of the weld joints were between 159-230 MPa and the % elongation values of the weld joints were between 2.28-5.44 %. The highest tensile strength value of 230.43 MPa was obtained from the specimen that was welded with the T16-S1000-F160 parameters. The lowest tensile strength value of 159.55 MPa was obtained from the specimen that was welded with the T16-S1000-F56 parameters. According to the optical microscope observations, the reason for the low tensile strength of the weld joint using these parameter values was caused by tunneling due to insufficient penetration. When Table 4 is examined, it is observed that the highest tensile strength values were obtained from the specimens that were welded with feed rate of 160 mm/min. It also can be seen in Table 4 that the lowest tensile strength values were obtained from the specimens welded with feed rate of 56 mm/min. Tensile test values show that feed rate is a factor that greatly affects welding performance of the welded plates. In order to make the effect of feed rate on weld joint strength more understandable, graphs of feed rate, yield and tensile strength values and % elongation were created while the tool shoulder diameter and spindle speed values kept constant.

The tensile test graphs obtained from the specimens welded with the use of 16 mm tool shoulder diameter are shown in Fig. 4, Fig. 5 and Fig. 6.

Table 4. Yield strength, Tensile strength and % Elongation average values of the Tensile Test

Parameter code	Yield strength (MPa)	Tensile strength (MPa)	Elongation (%)
1-T16-S710-F56	202.76	209.43	3.81
2-T16-S710-F112	205.21	219.73	4.97
3-T16-S710-F160	217.34	223.49	4.61
4-T16-S1000-F56	136.63	159.55	2.28
5-T16-S1000-F112	205.61	213.18	3.76
6-T16-S1000-F160	216.28	230.43	5.44
7-T16-S1400-F56	204.08	207.04	4.12
8-T16-S1400-F112	209.96	212.53	4.33
9-T16-S1400-F160	211.04	228.92	5.24
10-T20-S710-F56	198.53	201.11	4.06
11-T20-S710-F112	200.78	209.36	4.47
12-T20-S710-F160	206.75	217.13	4.82
13-T20-S1000-F56	197.29	200.30	4.02
14-T20-S1000-F112	202.48	206.92	4.24
15-T20-S1000-F160	207.86	220.81	4.95
16-T20-S1400-F56	155.16	193.62	4.38
17-T20-S1400-F112	201.80	212.63	5.02
18-T20-S1400-F160	208.34	221.05	4.92
19-T24-S710-F56	195.17	196.43	4.19
20-T24-S710-F112	197.67	200.96	4.29
21-T24-S710-F160	206.29	213.98	4.49
22-T24-S1000-F56	200.71	206.65	4.58
23-T24-S1000-F112	201.60	211.05	4.84
24-T24-S1000-F160	210.37	225.81	5.23
25-T24-S1400-F56	197.23	200.58	4.17
26-T24-S1400-F112	199.47	207.80	4.28
27-T24-S1400-F160	201.59	214.76	4.93

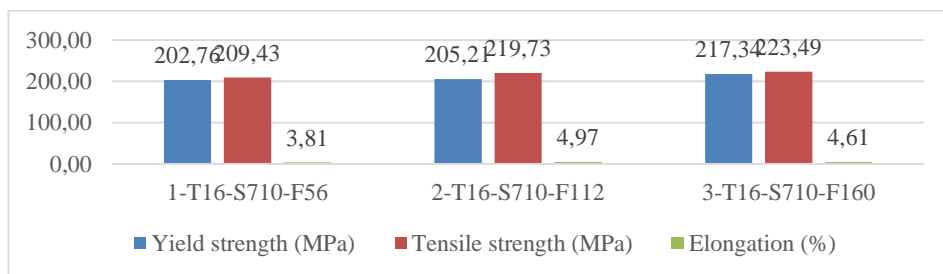


Figure 4. Tensile test graphs of specimens welded with 16 mm tool shoulder diameter and 710 rpm spindle speed parameter values

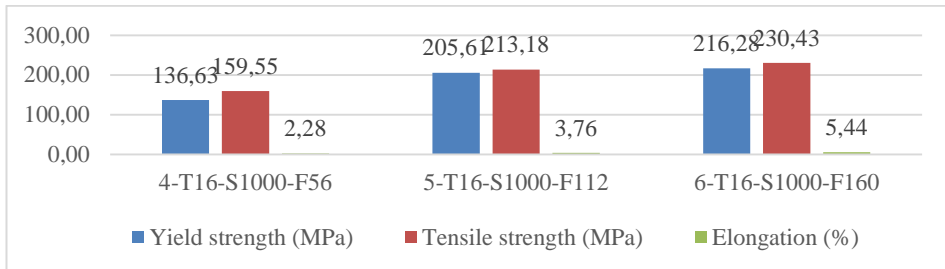


Figure 5. Tensile test graphs of specimens welded with 16 mm tool shoulder diameter and 1000 rpm spindle speed parameter values

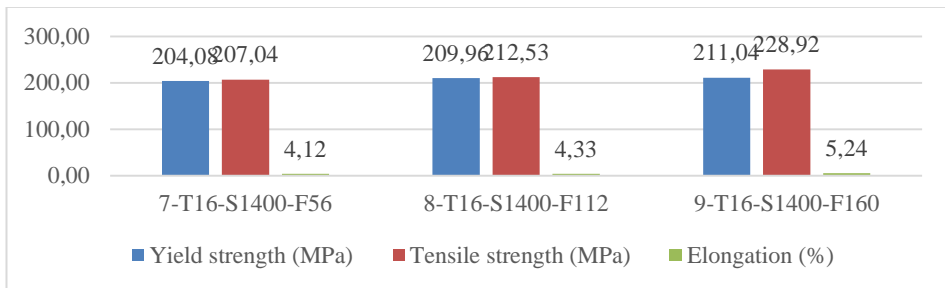


Figure 6. Tensile test graphs of specimens welded with 16 mm tool shoulder diameter and 1400 rpm spindle speed parameter values

Welded joints made using a 16 mm tool shoulder also showed an increase in weld strength as a result of the increased tool feed rate. The lowest tensile strength values were obtained from the specimens welded with feed rate of 56 mm/min and 1000 rpm spindle speed (Fig. 5). Among the parameters used with the tool shoulder diameter of 16 mm, the best weld strength was obtained with the use of medium rotational speeds and high feed rates (Fig. 5). In weld joints made with tool shoulder diameters of 20 and 24 mm, the tensile test values obtained showed similar results with that of 16 mm tool shoulder diameter weld joints which also show the conclusion that the increase in feed rate causes higher strength of the weld joints.

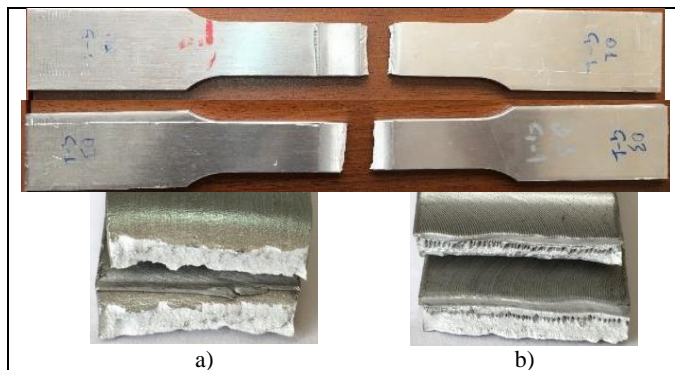


Figure 7. Visuals of fractured specimens after the tensile tests a) 1-T16-S710-F56 coded specimen, b) 3-T16-S710-F160 coded specimen

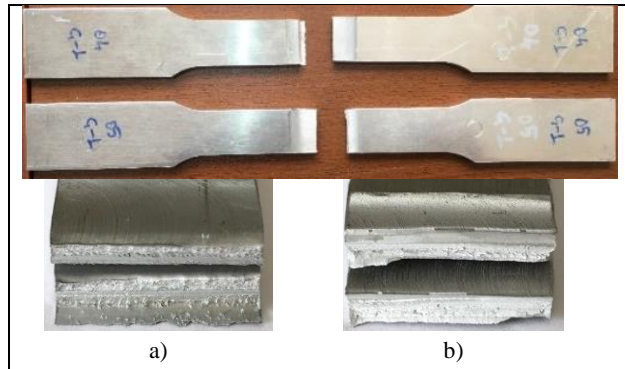


Figure 8. Visuals of fractured specimens after the tensile tests a) 4-T16-S1000-F56 coded specimen, b) 5-T16-S1000-F112 coded specimen

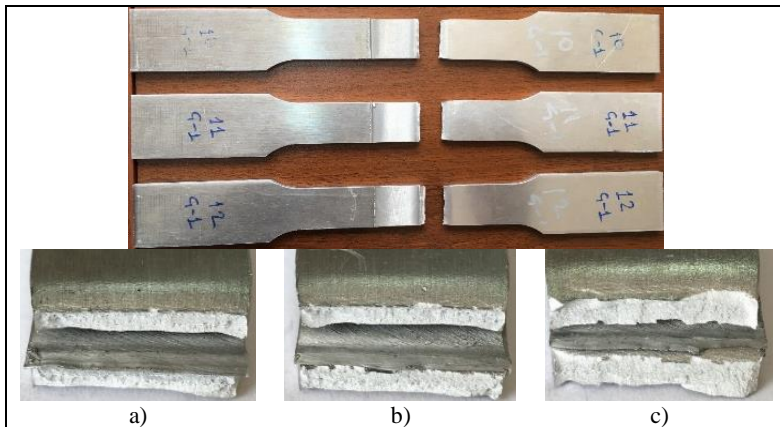


Figure 9. Visuals of specimens fractured at weld areas of EN AW-6082 aluminum alloy a) 10-T20-S710-F56 coded specimen, b) 11-T20-S710-F112 coded specimen, c) 12-T20-S710-F160 coded specimen

After the examination of the fractured specimens following the tensile tests, except the specimens with the codes 2-T16-S710-F56, 3-T16-S710-F160, 4-T16-S1000-F56 and 5-T16-S1000-F112 (Figs. 7-8), all the specimens were fractured in the EN AW-6082 aluminum alloy base metal zone (Fig. 9). When the fracture zones of the specimens were examined after the tensile tests, it was observed that the damage generally occurred in the TMAZ of the EN AW-6082 aluminum alloys. This is caused by the internal hardening of the 6082 alloy during the recrystallization process which causes decrease in strength at TMAZ, which has been specified in other studies in the literature [33]. The SEM images of the 6-T16-S1000-F160 parameter coded specimen, having the highest tensile strength value among all the parameters employed, are given in Fig. 10. When these images are examined, a 5-10 μm wide homogenous porous grain structure was observed. This homogenous porous grain structure was formed due to the increase in grain boundaries and provided high strength properties in the specimen [34-36].

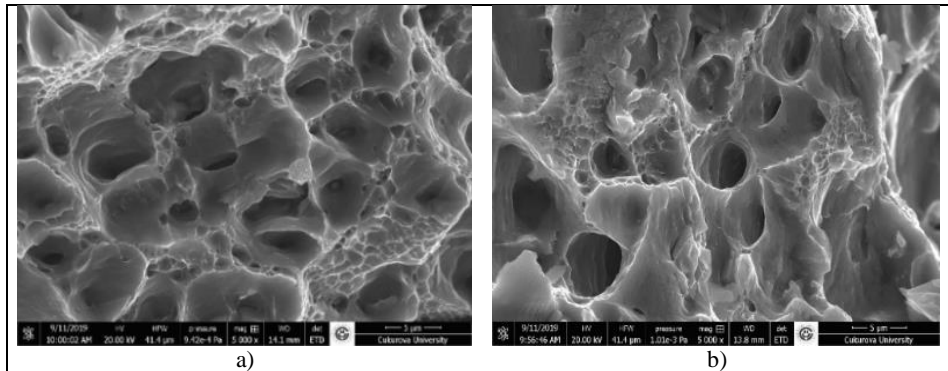


Figure 10. Weld zone SEM fractographs of the 6-T16-S1000-F160 coded specimens (Magnified 5000 X) a) EN AW-5083 alloy side b) EN AW-6082 alloy side

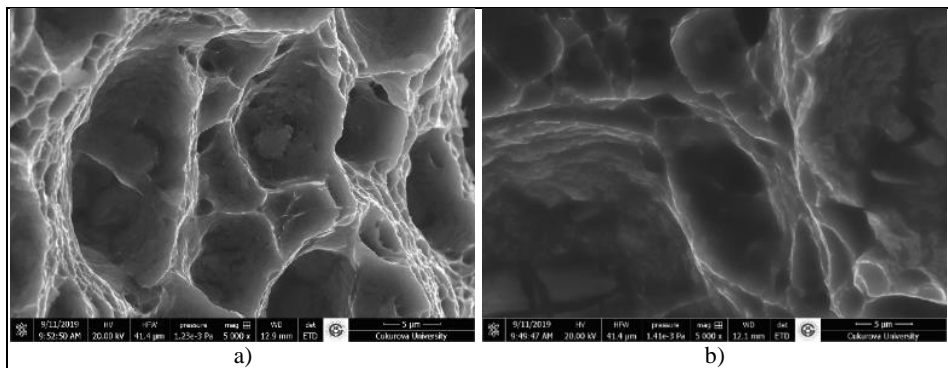


Figure 11. Weld zone SEM fractographs of the 4-T16-S1000-F56 coded specimens (Magnified 5000 X) a) EN AW-5083 alloy side b) EN AW-6082 alloy side

When the SEM images of the fracture surface are taken from the EN AW-5083 region after the tensile test of the combined sample in the 4-T16-S1000-F56 parameter, a porous grain and irregular structure are examined. This porous structure emerged due to the reduction of grain boundaries and caused the welded joint to show low strength properties. When the SEM images of the fracture surface taken from the EN AW-6082 region are examined, it is seen that an irregular structure with a porous grain of 20 µm width is formed.

The chemical composition of the weld area was determined with the use of Energy-dispersive X-ray spectroscopy (EDS) method. The EDS analysis results for the 6-T16-S1000-F160 specimen which was fractured at weld area of EN AW-6082 side are given in Fig. 12.

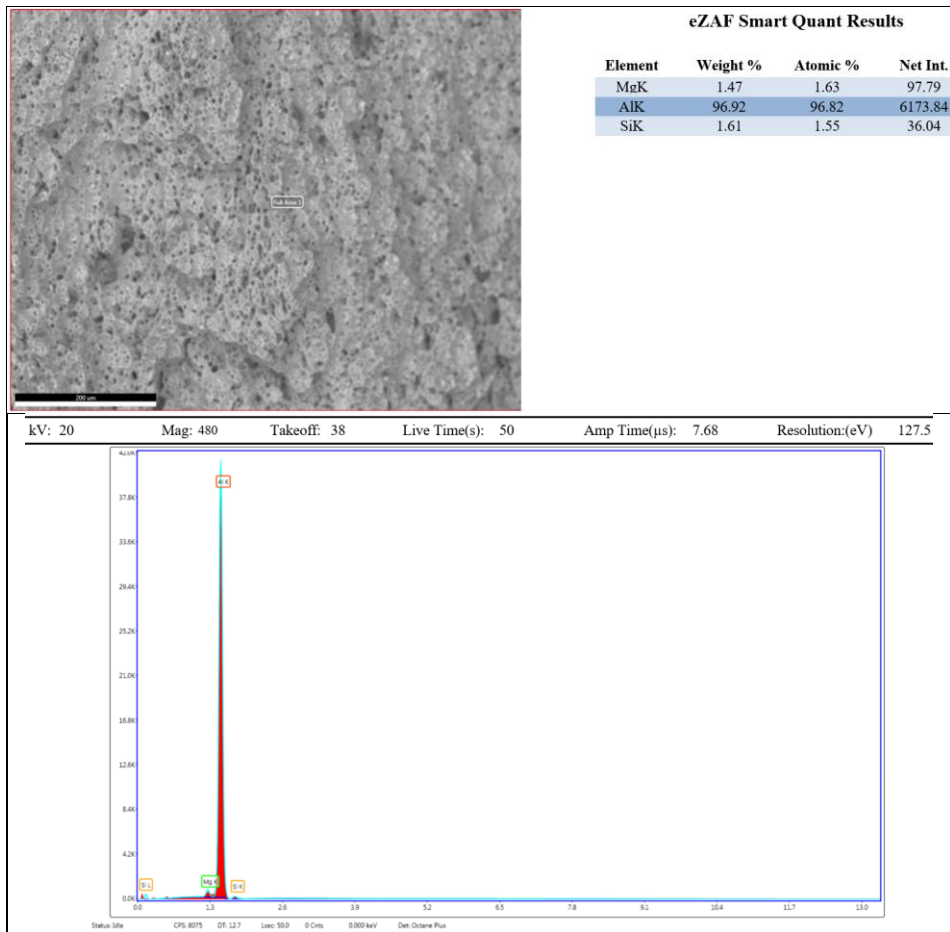


Figure 12. EDS analysis results of 6-T16-S1000-F160 coded specimen

According to the EDS results, no elements or compounds other than that of the base metals were detected. The element content of the weld fracture area showed similar properties with the EN AW-6082-T651 alloy.

3.2 Findings of micro hardness examination

The hardness value of EN AW-5083 base metal was measured as 92.46 HV and the hardness value of EN AW-6082 base metal was measured as 123.30 HV. The highest hardness value was measured as 107.40 HV at the TMAZ of welds joined with the use of 16 mm tool shoulder diameter and with the parameters used in 3-T16-S710-F160 specimen with 710 rpm spindle speed and 160 mm/min feed rate (Fig. 13).

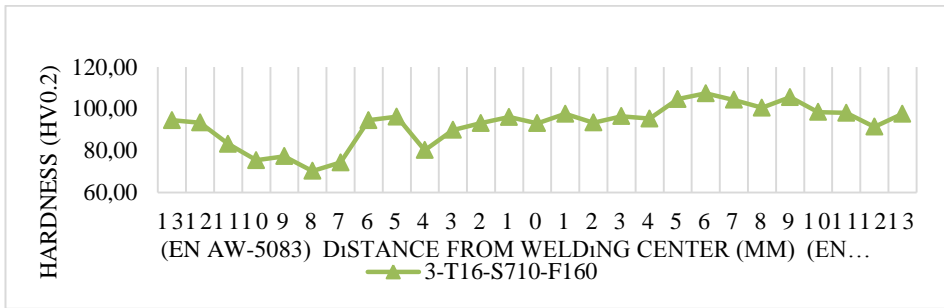


Figure 13. Micro hardness measurement graph of the 3-T16-S710-F160 parameter coded specimen

The highest hardness value was measured as 117.7 HV at the TMAZ of welds joined with the use of 20 mm tool shoulder diameter and with the parameters used in 12-T20-S710-F160 specimen with 710 rpm spindle speed and 160 mm/min feed rate (Fig. 14).

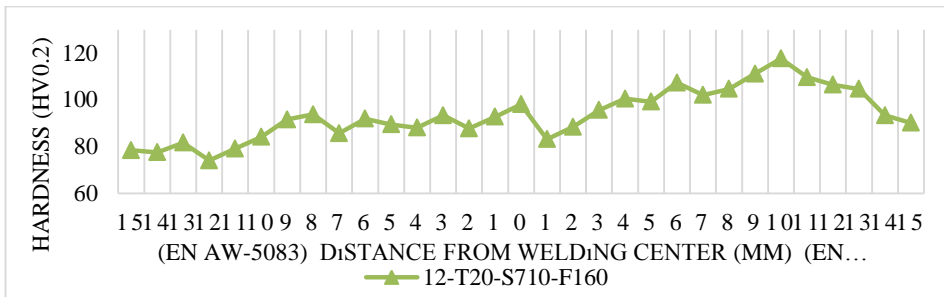


Figure 14. Micro hardness measurement graph of the 12-T20-S710-F160 parameter coded specimen

The highest hardness value was measured as 115.1 HV at the TMAZ of welds joined with the use of 24 mm tool shoulder diameter and with the parameters used in 21-T24-S710-F160 specimen with 710 rpm spindle speed and 160 mm/min feed rate (Fig. 15).

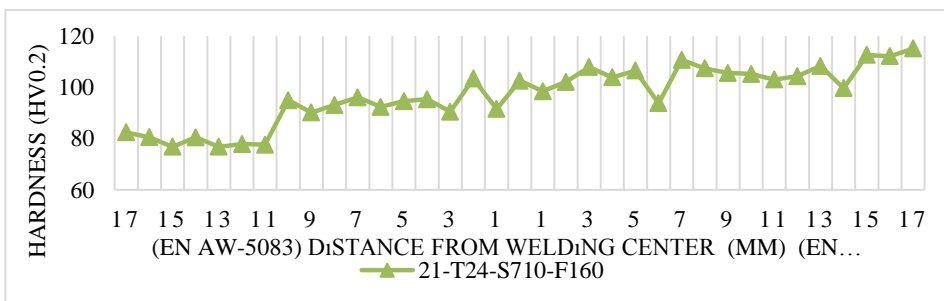


Figure 15. Micro hardness measurement graph of the 21-T24-S710-F160 parameter coded specimen

The micro hardness values at the weld joints were found to be lower than the hardness value of the EN AW-6082 base metal. In the majority of the welded areas the hardness values were high at the EN AW-6082 base metal side and the hardness values were low at the EN AW-5083 base metal side. The hardness values for all specimens are given in Fig. 16, Fig. 17 and Fig. 18. When joining different Al alloys with FSW method, it was seen that the hardness values are related to the amount of deformation and the strength of the base metals. Therefore, an asymmetrical hardness profile is formed between the EN AW-5083 base metal and the EN AW-6082 base metal in the welded zone.

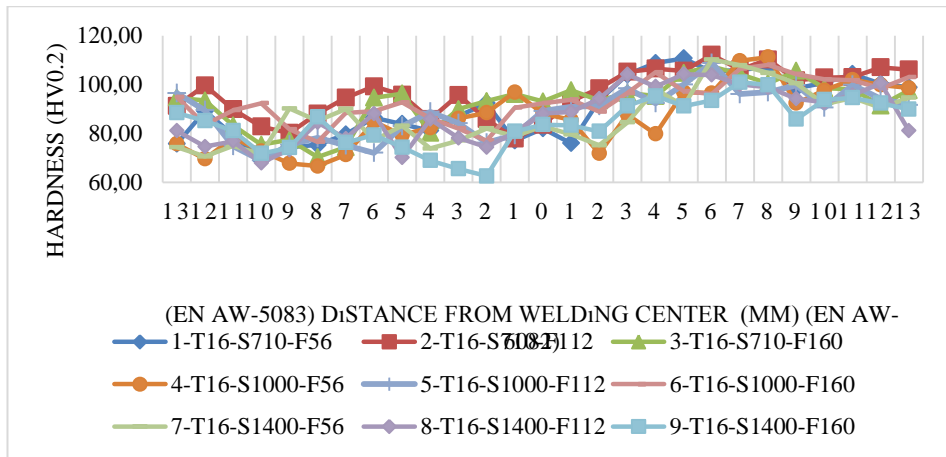


Figure 16. Hardness values of specimens combined with tool shoulder diameter of 16 mm

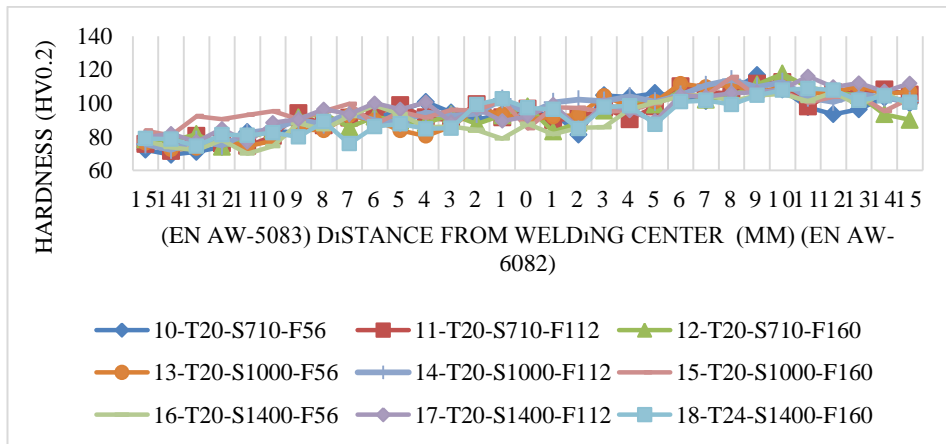


Figure 17. Hardness values of specimens combined with tool shoulder diameter of 20 mm

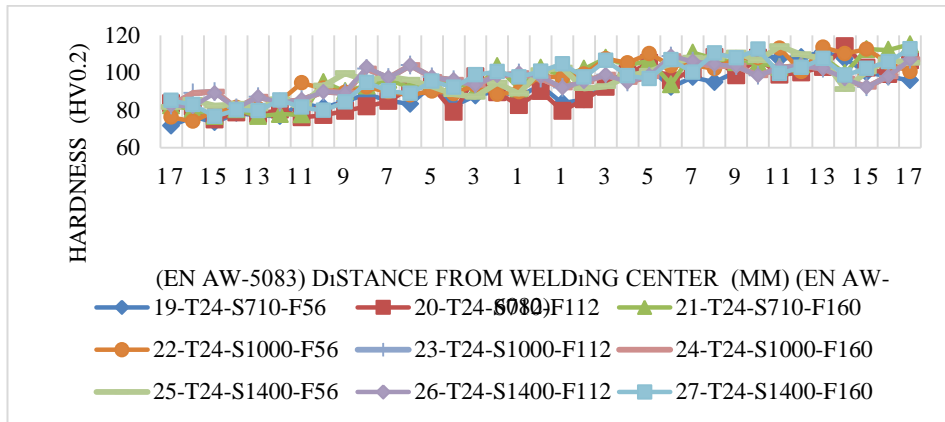


Figure 18. Hardness values of specimens combined with tool shoulder diameter of 24 mm

4. CONCLUSION

In this study two aluminum alloy plates of EN AW-5083-H111 and EN AW-6082-T651 were joined with Friction Stir Welding method. Weld joints were obtained by using 27 various parameters composed of three different tools of different shoulder diameters of 16-20-24 mm, spindle speeds of 710-1000-1400 rpm and feed rates of 56-112-160 mm/min. Test specimens complying with the test standards were prepared from the weld joints of the welded plates and the mechanical properties, metallographic investigations and hardness values were of the joints were examined. In the tensile tests the highest tensile strength values were obtained from the specimens that were welded with parameters having the feed rate of 160 mm/min. On the other hand, the lowest tensile strength values were obtained from the specimens that were welded with parameters having the feed rate of 56 mm/min. In general, the increase in feed rate caused improvement in the tensile strength and yield strength of the weld joints during FSW process. In general, the micro hardness values at the weld joints were observed to be lower than that of the EN AW-6082 base metal. In the majority of the welded areas the hardness values were high at the EN AW-6082 base metal side and the hardness values were low at the EN AW-5083 base metal side. Generally the average hardness values measured at the center of the weld areas increased in parallel with the increase in the tool shoulder diameters and feed rates. As a result of the tensile test, the rupture zones occurred in the welded center (weld nugget) and TMAZ. It is thought that the change in the hardness values and the loss of strength of these regions are due to inhomogeneous mixing and micro-porosity formation.

REFERENCES

- [1] Kulekci, M., K., Şik A., Kaluç, E. (2008). Effects of tool rotation and pin diameter on fatigue properties of friction stir welded lap joints, *International Journal of Advanced Manufacturing Technology*, Vol. 36, 877-882, doi: 10.1007/s00170-006-0901-z.
- [2] Oates, W.R. (Ed.). (1998). *Welding Handbook-Materials and Applications*, AWS, 8th Edition.
- [3] What is Welding?-Definition, processes and types of joints, from <https://www.twi-global.com/technical-knowledge/faqs/what-is-welding>, accessed September 15, 2019.
- [4] Kaynak Tekniği El Kitabı-Yöntemler Ve Donanımlar, Anık, S. (1991), from http://www.gedikigitimvakfi.org.tr/wp-content/uploads/2013/12/library_6.pdf, accessed September 15, 2019.

- [5] Hou, K., Baeslack, W. (1996). Characterization of the heat-affected zone in gas tungsten arc welded aluminium alloy 2195-T8, *Journal of Materials Science Letters*, Vol. 15, No. 3, 239–244, doi:10.1007/BF00274462.
- [6] Koteswara Rao, S.R., Madhusudhan Reddy, G., Srinivasa Rao, K., Kamaraj, M., Prasad Rao, K. (2005). Reasons for superior mechanical and corrosion properties of 2219 aluminum alloy electron beam welds, *Materials Characterization*, Vol. 55, No. 4-5, 345–354, doi: 10.1016/j.matchar.2005.07.006.
- [7] Paston, M., Zhao, H., Martukannitz, R.P., Debroy, T. (1999). Porosity, underfill and magnesium loss during continuous wave Nd: YAG laser welding of thin plates of aluminium alloy 5182 and 5754, *Materials Science*, 207–216.
- [8] Yeniyil, E., Boga, C., Eşme, U. (2019). Effects of ultrasonic welding parameters for solar collector applications, *Materials Testing*, Vol. 61, No. 4, 344-348, <https://doi.org/10.3139/120.111326>.
- [9] Klobcar, D., Kosce, L., Pietras, A., Smolej, A. (2012). Friction-stir welding of aluminium alloy 5083, *Materials and Technology*, Vol. 46, No. 5, 483–488.
- [10] Industrial Applications, from <https://www.twi-global.com/what-we-do/research-and-technology/technologies/welding-joining-and-cutting/friction-welding/friction-stir-welding/industrial-applications>, accessed September 22, 2019.
- [11] New joining technologies for future fuselage metal structures, from https://www.iws.fraunhofer.de/content/dam/iws/en/documents/publications/annual_report_articles/JB_IWS_2014_en_S30-31.pdf, accessed September 22, 2019.
- [12] Besharati-Givi, M.K., Asadi, P. (2014). *Advances in Friction-Stir Welding and Processing*, Woodhead Publishing.
- [13] James, M.N., Hattingh, D.G., Bradley, G.R. (2003). Weld tool travel speed effects on fatigue life of friction stir welds in 5083 aluminium, *International Journal of Fatigue*, Vol. 25, 1389-1398, doi: 10.1016/S0142-1123(03)00061-6.
- [14] Kumar, R., Singh, K., Pandey S. (2012). Process forces and heat input as function of process parameters in AA5083 friction stir welds, *Trans. Nonferrous Met. Soc. China*, Vol. 22, 288-298, doi: 10.1016/S1003-6326(11)61173-4.
- [15] Cavaliere, P., Squillace, A., Panella, F. (2008). Effect of welding parameters on mechanical and microstructural properties of AA6082 joints produced by friction stir welding, *Journal of Materials Processing Technology*, Vol. 200(1-3), 364–372, doi: 10.1016/j.jmatprotec.2007.09.050.
- [16] Mroczka, K., Pietras, A. (2009). FSW characterization of 6082 aluminium alloys sheets, *Archives of Materials Science and Engineering*, Vol. 40, 104-109.
- [17] Costa, J.D., Ferreira, J.A.M., Borrego, L.P., Abreu, L.P. (2012). Fatigue behaviour of AA6082 friction stir welds under variable loadings, *International Journal of Fatigue*, Vol. 37, 8-16, doi: 10.1016/j.ijfatigue.2011.10.001.
- [18] El-Danaf E.A., El-Rayes M.M. (2013). Microstructure and mechanical properties of friction stir welded 6082 AA in as welded and post weld heat treated conditions, *Materials and Design*, Vol. 46, 561-572, doi: 10.1016/j.matdes.2012.10.047.
- [19] El-Rayes, M.M., El-Rayes, M.M. (2012). The influence of multi-pass friction stir processing on the microstructural and mechanical properties of Aluminum Alloy 6082, *Journal of Materials Processing Technology*, Vol. 212, 1157-1168, doi: 10.1016/j.jmatprotec.2011.12.017.
- [20] Cabibbo, M., Forcellese, A., El Mehtedi, M., Simoncini M. (2014). Double side friction stir welding of AA6082 sheets: microstructure and nanoindentation characterization, *Materials Science & Engineering A*, Vol. 590, 209-217, doi:10.1016/j.msea.2013.10.031.

- [21] Krasnowski, K., Hamilton, C., Dymek, S. (2015). Influence of the tool shape and weld configuration on microstructure and mechanical properties of the Al 602 alloy FSW joints, *Archives of Civil and Mechanical Engineering*, Vol. 15, 133-141, <https://doi.org/10.1016/j.acme.2014.02.001>.
- [22] Cho, J.H., Kim, W.J., Lee C.G. (2014). Evolution of microstructure and mechanical properties during friction stir welding of A5083 and A6082, *Procedia Engineering*, Vol. 81, 2080-2085, <https://doi.org/10.1016/j.proeng.2014.10.289>.
- [23] Singha J., Shankar, L. (2015). Analysis of process parameters effect on friction stir welding of aluminium 5083 and 6082, *Iracst- International Journal of Research in Management & Technology*, Vol. 5, 2249-9563.
- [24] Gungor, B., Kaluc, E., Taban, E., Sik, A. (2014). Mechanical, fatigue and microstructural properties of friction stir welded 5083-H111 and 6082-T651 aluminum alloys, *Materials and Design*, Vol. 56, 84-90, <https://doi.org/10.1016/j.matdes.2013.10.090>.
- [25] Zucchi, F., TrabANELLI, G., Grassi, V. (2001). Pitting and stress corrosion cracking resistance of friction stir welded AA5083, *Materials and Corrosion*, Vol. 52, 853-859, [https://doi.org/10.1002/1521-4176\(200111\)52:11<853::AID-MACO853>3.0.CO;2-1](https://doi.org/10.1002/1521-4176(200111)52:11<853::AID-MACO853>3.0.CO;2-1).
- [26] Vilaca, P., Pepe, N., Quintino, L. (2006). Metallurgical and corrosion features of friction stir welding of AA5083-H111, *Welding in the World*, Vol. 50, No. 9-10, 55-64.
- [27] Park, S., Kim, J., Han, M., Kim, S. (2009). Corrosion and optimum corrosion protection potential of friction stir welded 5083-O Al alloy for leisure ship, *Trans. Nonferrous Met. Soc. China*, Vol. 19, No. 4, 898-903, [https://doi.org/10.1016/S1003-6326\(08\)60373-8](https://doi.org/10.1016/S1003-6326(08)60373-8).
- [28] Shen, C., Zhang, J., Ge, J. (2011). Microstructures and electrochemical behaviors of the friction stir welding dissimilar weld, *Journal of Environmental Sciences*, Vol. 23, 32-35, [https://doi.org/10.1016/S1001-0742\(11\)61072-3](https://doi.org/10.1016/S1001-0742(11)61072-3).
- [29] Patil, H.S., Soman, S.N. (2014). Corrosion behaviour of friction stir welded aluminium alloys AA6082-T6, *American Journal of Materials Engineering and Technology*, Vol. 2, 29-33, doi:10.12691/materials-2-3-1.
- [30] Donatus, U., Thompson, G.E., Zhou, X., Wang, J., Cassell, A., Beamish, K. (2015). Corrosion susceptibility of dissimilar friction stir welds of AA5083 and AA6082 alloys, *Materials Characterization*, Vol. 107, 85-97, doi: 10.1016/j.matchar.2015.07.002.
- [31] Referans Metal, from <http://referansmetal.com/alasimli-aluminyum/list/4/genel-endustri>, accessed September 30, 2019.
- [32] Empo Alüminyum, from <http://www.empo.com.tr/aluminyum-lama-ve-cubuk/en-aw-6082.html>, accessed September 30, 2019.
- [33] E. Taban, E., Kaluç, E. (2004). Alüminyum ve Alüminyum Alaşımlarının Sürtünen Eleman ile Birleştirme Kaynağında (FSW) Kaynak Bölgesinin Mikroyapısal Özellikleri, *Metal Dünyası*, Vol. 136, 131-140.
- [34] Fouladi, S., Ghasemi, A H., Abbasi, M., Abedini, M., Khorasani, A.M., Gibson, I. (2017). The effect of vibration during friction stir welding on corrosion behavior, mechanical properties, and machining characteristics of stir zone, *Metals*, Vol. 7, No.10, 1-14, <https://doi.org/10.3390/met7100421>.
- [35] Naderi, M., Abbasi, M., Saeed-Akbari, A. (2013). Enhanced mechanical properties of a hot-stamped advanced high-strength steel via tempering treatment, *Metall. Mater. Trans. A*, Vol. 44, 1852–1861, doi: 10.1007/s11661-012-1546-1.
- [36] Ma, Z., Pilchak, A., Juhas, M., Williams, J. (2008). Microstructural refinement and property enhancement of cast light alloys via friction stir processing, *Scr. Mater.*, Vol. 58, 361–366, doi: <https://doi.org/10.1016/j.scriptamat.2007.09.062>.